Sensor and Simulation Notes

Note 443

March 2000

Design, Fabrication and Measurement of a Conical Transmission-Line Fed, Cassegrain Coaxial Beam-Rotating Antenna

Clifton C. Courtney, Donald E. Voss and David Slemp
Voss Scientific
Albuquerque, NM

Carl E. Baum, Robert Torres and William Prather
Air Force Research Laboratory / Directed Energy Directorate
Kirtland Air Force Base, NM

ABSTRACT

The design of a Conical Transmission-Line Fed, Cassegrain Coaxial Beam-Rotating Antenna is summarized, and the implementation of the design and fabrication of a prototype antenna, the COBRA III, is reviewed. The COBRA III prototype antenna uses a Cassegrain-type configuration with a paraboloidal main reflector and a hyperboloidal subreflector. The feed structure consists of a conical coaxial transmission line that has its vertex at the vertex of the paraboloidal reflector, and whose center conductor attaches directly to the subreflector. The results of measurements taken to determine the circuit and radiating properties of the COBRA III prototype are also presented. These include measurements of the antenna input impedance, the radiated pattern and gain for several antenna configurations (N = 1, N = 2, N = 4), and the bandwidth (gain, input impedance, boresight gain and phase of orthogonal field components) characteristics of the antenna. The measurements show that the pattern, gain, aperture efficiency, polarization and bandwidth characteristics of the COBRA III are superior to earlier COBRA prototypes that used conventional microwave horn feeds. It is also shown that the inherent SWR of the feed structure is 2.5 : 1 or less over the measured bandwidth (100 MHz – 6 GHz).

Acknowledgement - This work was supported in part by the Air Force Office of Scientific Research, and in part by the Air Force Research Laboratory, Directed Energy Directorate, under a Small Business Innovation for Research (SBIR) Phase II program, Contract No. F29601-97-C-0005.

Table of Contents

Table of Figures

Table of Tables

1. INTRODUCTION

The analysis, design, and optimization of a conical transmission line-fed, Cassegrain, Coaxial Beam-Rotating Antenna (COBRA) was presented in [Ref. 3, 13]. A summary of the design, details of the fabrication, and electrical measurements of a prototype antenna (COBRA III) are presented in this note. The COBRA III prototype antenna is the third in a line that uses structural adjustments of reflecting surfaces to modify the aperture distribution of an otherwise azimuthally symmetric aperture distribution to realize a boresight peak with linear or circular polarization. Whereas the previous antenna prototypes used circular aperture feed horns to illuminate the main reflector, the COBRA III prototype antenna uses the center conductor of a conical transmission line attached to a hyperboloidal subreflector as the antenna feed. The idea is simply that the transmission line field propagates along its extent, strikes the subreflector and is reflected, then illuminates the main reflector. As was the case with previous prototypes, the main reflector has been divided into four equal segments, and these segments are adjusted in the usual way [Ref. 1, 2] to produce a boresight peak with linear or circular polarization. A schematic diagram of the COBRA III, indicating the dimensions of the feed structure, is shown in Figure 1.

As indicated in the figure, the antenna feed of the COBRA III prototype is a pseudo-conical transmission line, where the vertex of the conical transmission line is at the vertex of the paraboloidal reflector. The conical transmission line has a nominal characteristic impedance of $Z_0 = 80\ \Omega$, based on the half angles of the inner and outer conductors of the transmission line. The inner conductor attaches directly to the subreflector and has a nominal diameter that extends just across the subreflector's shadow boundary. The outer conductor continues from the vertex, to a point—along the conical path—just before it intercepts the inner most ray path off of the subreflector (see figure). At this point the edge turns, and continues along a path parallel with the innermost ray path. It does not terminate on the main reflector, rather it stops abruptly at a point where it will clear all of moving surfaces of the main reflector.

The design of the conical transmission line feed system for the COBRA III [Ref. 3, 4] led to consideration of the question: What is the optimum system impedance (ratios of inner- to outer-conductor angles, ratios of subreflector to reflector diameter)? The answer to this questions depends on whether one wishes to maximize the physical aperture size to reduce electric field stresses [Ref. 5, 6], or maximize the boresight gain. For the COBRA III, we designed to optimize the boresight gain. The topics of this note are as follows: First, a summary of the design and fabrication of the conical transmission line-fed Coaxial Beam-Rotating Antenna (COBRA III) is given. Once fabrication was complete, a measurement program to determine the circuit and radiating characteristics of the COBRA III was undertaken. Measurements of the antenna's input impedance, and location of major impedance discontinuities in the transmission line feed via time domain analysis were conducted. Also, the azimuthal patterns of the COBRA III configured to radiate a boresight null (N = 1), a boresight peak with linear polarization (N = 2), and a boresight

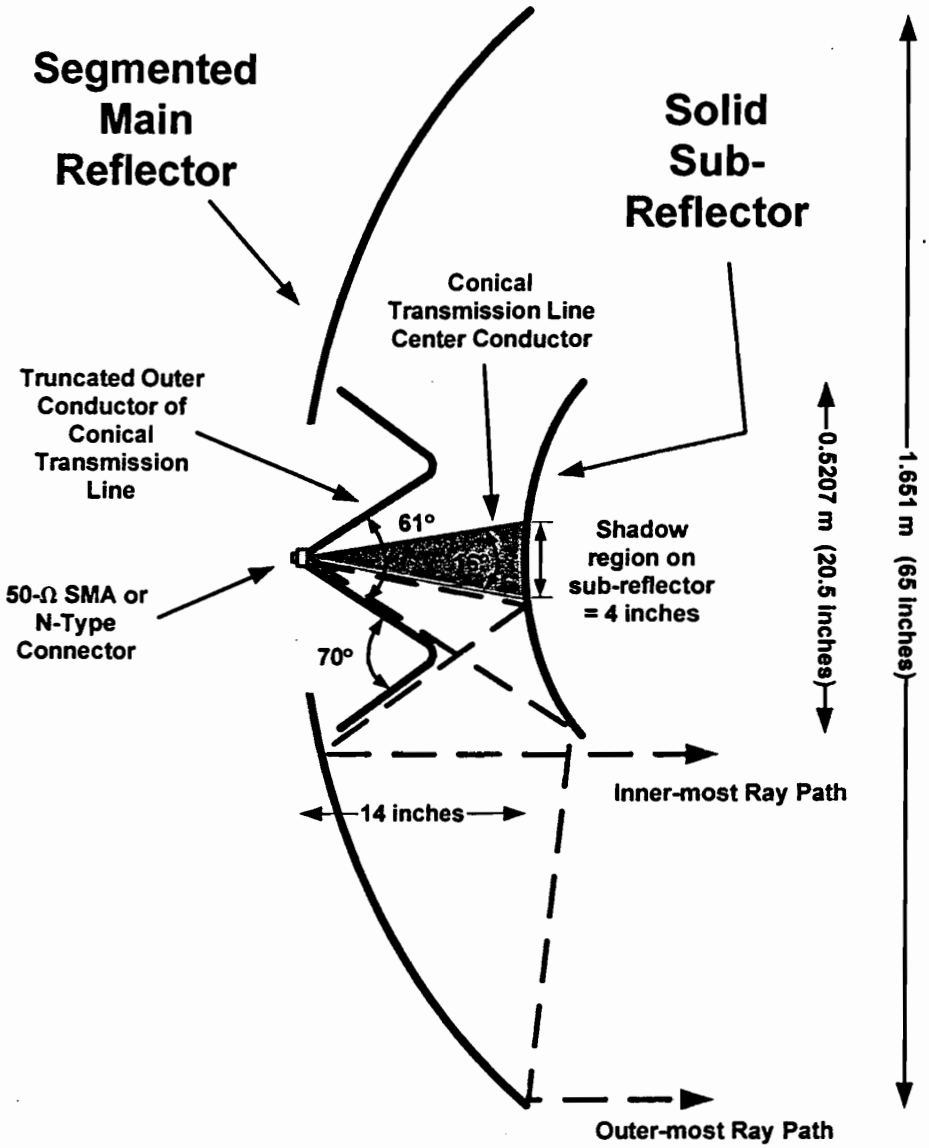

Figure 1. A schematic diagram of the COBRA III prototype.

peak with circular polarization (N = 4) were measured. Measurements of the frequency dependence of the boresight gain also were made for these COBRA III configurations. All measurements were made with the COBRA III configured for a center frequency of $_0$ 3 GHz. Also, measurements of the boresight gain and phase response in reception of the COBRA III subjected to vertically and horizontally polarized incident fields were made for the N = 4 (circular polarization) configuration. The results of these measurements are reported here. Finally, a summary of the operating characteristics of the COBRA III is given, along with comparisons to the measured characteristics of the COBRA II, which utilizes a more conventional conical horn feed. Comments on the design and measurement of the COBRA III, and suggestions for future research conclude this note.

2. COBRA III DESIGN SUMMARY

The COBRA III operates by utilizing the same fundamental principles exploited in earlier COBRA prototypes [Ref. 1]. Generally, when an azimuthally symmetric field illuminates a paraboloidal reflector, the resulting radiated field will exhibit a boresight null. To change this result, we have shown previously that a paraboloidal reflector can be segmented in such a way to allow variation of the round trip distance from the focal point of the reflector, to the reflector's aperture plane. Accomplished through a combination of translation and rotation of reflector segments, this variation transforms the azimuthally symmetric field to an aperture distribution that exhibits a boresight peak with linear or horizontal polarization. A thorough discussion of these concepts along with detailed analysis of the approach is found in the literature [Ref. 1, 2, 3, 4, 9]. A summary of the physical characteristics of the COBRA III prototype is presented next.

2.1 Main Paraboloidal Reflector

The main reflector is a paraboloidal surface with an usable diameter of 62.5 inches, and a focal length to diameter ratio of 0.25 (see Figure 2 and Figure 3a). It has been partitioned into four equal segments (petals), with individual petal control and positioning (Figure 3b). The COBRA III prototype uses the same segmented paraboloidal reflector and segment control mechanisms used with the COBRA II. The reflector and control mechanisms are described in detail in [Ref. 2]. The principle parameters associated with the paraboloidal reflector are summarized in Table 1.

2.2 Subreflector

The subreflector is a hyperboloidal surface with its convex side facing the main reflector, and its prime focus located at the prime focus of the main paraboloidal reflector (see Figure 2 and Figure 3b). Its conjugate focus is located at the vertex of the main reflector. Its axis is coincident with the axis of the main reflector, and its apex (the point on the subreflector closest to the main reflector) is 14 inches from the vertex of the main reflector. The subreflector's eccentricity is 1.623, which places the prime focus of the main reflector and the subreflector 2 inches behind the apex of the subreflector. The subreflector diameter is slightly oversized at 20.5 inches. The shadow region on the subreflector (the inner diameter of the subreflector for which rays are blocked by the subreflector as they reflect off the main reflector) is approximately 4 inches. The COBRA III prototype uses the same hyperboloidal subreflector used with the COBRA II [Ref. 2]. The principle parameters associated with the subreflector are summarized in Table 1.

Table 1. Summary of COBRA III reflector / subreflector parameters.

Paraboloidal reflector diameter	62.5 inches = 158.75 cm
Paraboloidal reflector focal length	0.25
Focal length to diameter ratio	0.25
Number of segments in paraboloidal reflector	4
Subreflector surface	hyperboloidal
Subreflector eccentricity	1.623
Subreflector diameter	20.5 inches = 52.07 cm
Subreflector shadow diameter	4 inches = 10.16 cm

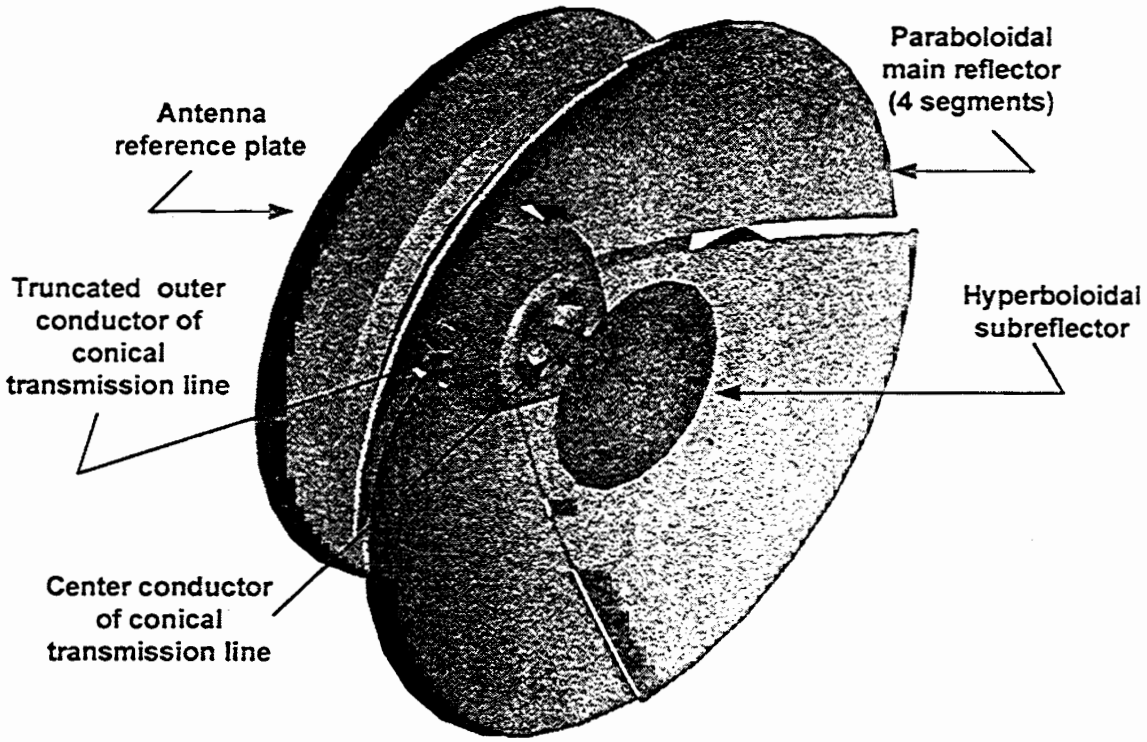

Figure 2. **A schematic rendering of the COBRA III prototype antenna in the $N = 4$ configuration is shown. The inner and outer conductors of the conical transmission line feed are depicted, as well as the outer conductor collar.**

(a)

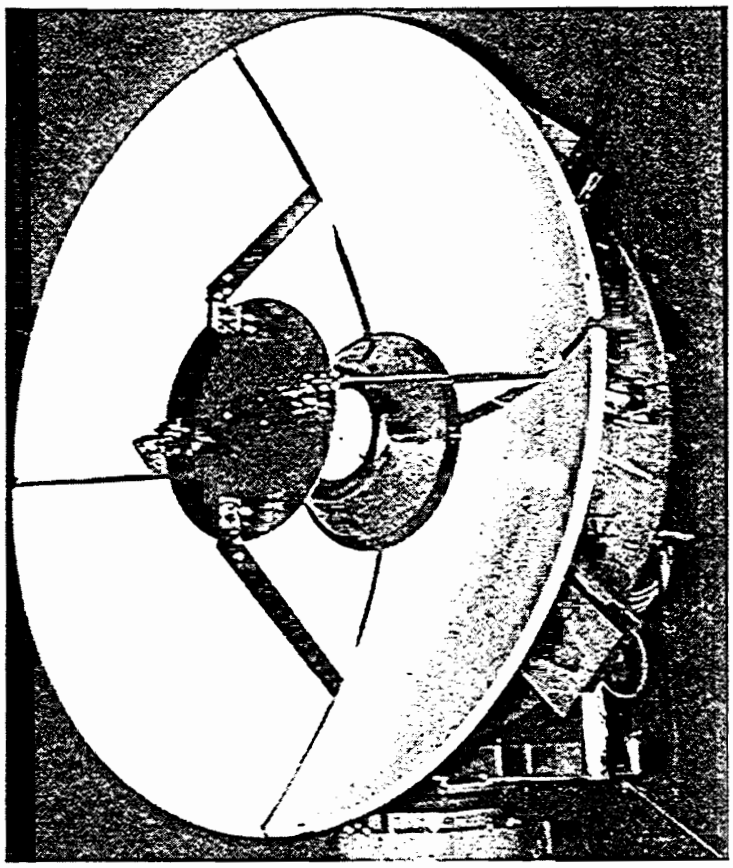

(b)

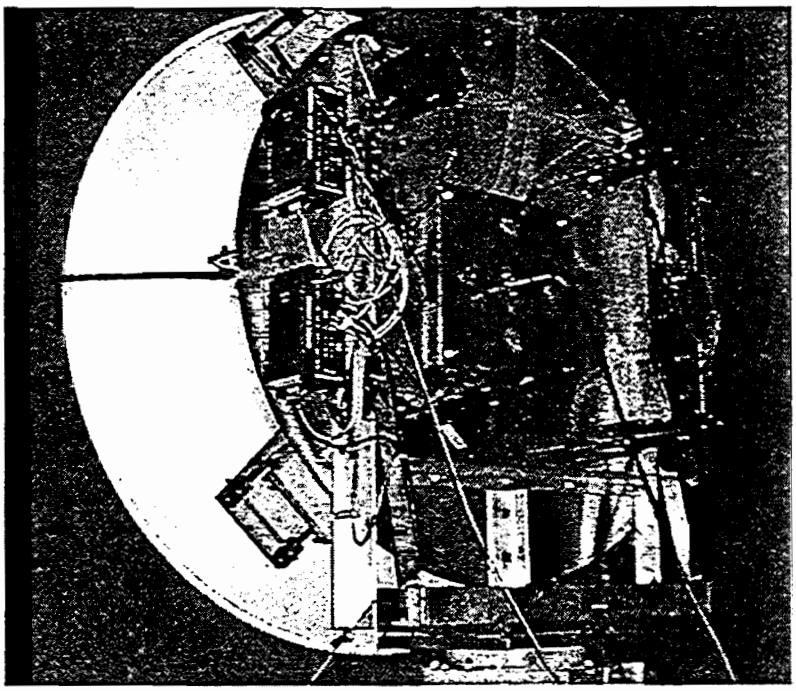

Figure 3. **The COBRA III Prototype: (a) view from the front showing segmented main reflector and conical feed; and (b) view from the rear showing base plate and petal control mechanisms.**

2.3 COBRA III Feed Geometry

The RF feed point for the COBRA III is an N-type, 50-Ω connector mounted on a conical transmission line base plate. The base plate is unique to the COBRA III and is located the behind the antenna reference plate. The N-type connector feed of the COBRA III is shown in Figure 5. Just beyond the N-type connector the transmission line abruptly changes geometry from a cylindrical coaxial to conical coaxial geometry. The impedance also jumps discontinuously at this point from $Z_0 = 50\Omega$ to $Z_0 = 80\ \Omega$, defined by the impedance of the conical coaxial transmission line (see Figure 6) with half angles of the inner and outer conductors of

$$\theta_1 = \arctan\left(\frac{4/2}{14}\right) = 8.13^o.$$

and

$$\theta_2 = \arctan\left(\frac{20.5/2}{14+3.5}\right) = 30.35^o.$$

The resulting conical transmission line impedance is then

$$Z_0 = \frac{377}{2\pi}\ln\left[\frac{\cot(\theta_1/2)}{\cot(\theta_2/2)}\right] = \frac{377}{2\pi}\ln\left[\frac{\cot(8.12/2)}{\cot(30.35/2)}\right] = 80.4\Omega$$

Note that the conical transmission line impedance of $Z_0 = 80\Omega$ is consistent with the system impedance criteria for peak gain: $Z_{System}^{Peak\ Gain} = 75\Omega$. Again, we were motivated to design the feed with these values to demonstrate the proposed antenna concepts and to optimize the peak boresight gain, rather than to minimize the system's peak electric field. A desire to minimize the electric field would result in the selection of a different system impedance [Ref. 3, 4].

A close-up view of the principle components of the coaxial conical transmission line feed is presented in Figure 4. The truncated outer conductor is shown as it folds back to follow the innermost ray not blocked by the subreflector. Supported by a Styrofoam insert, the center conductor can be seen exiting through the truncated transmission line aperture. In the picture, it is apparent how the center conductor attaches to the subreflector. The seams in the main reflector, and the subreflector supporting struts, are also visible in the figure.

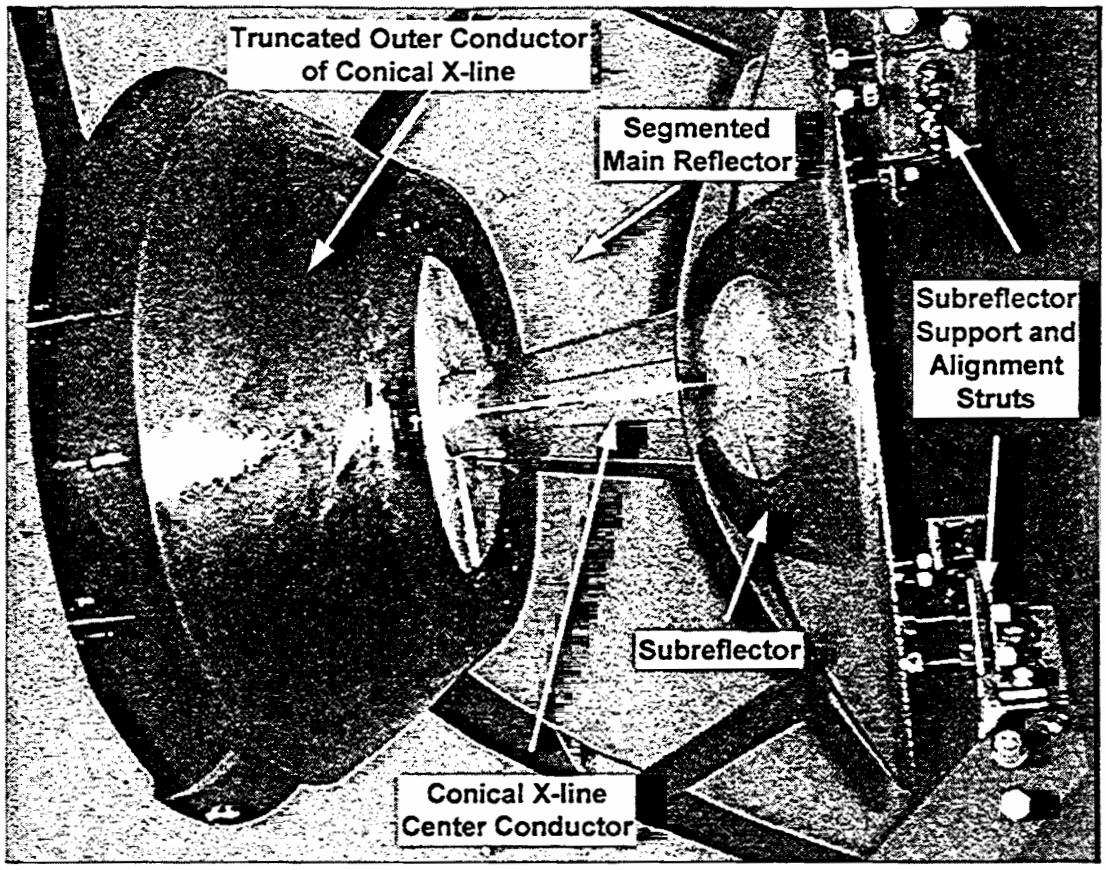

Figure 4. **The conical feed system of the COBRA III. Shown are the truncated outer conductor and inner conductor of the conical feed x-line, the segmented main reflector, and the subreflector.**

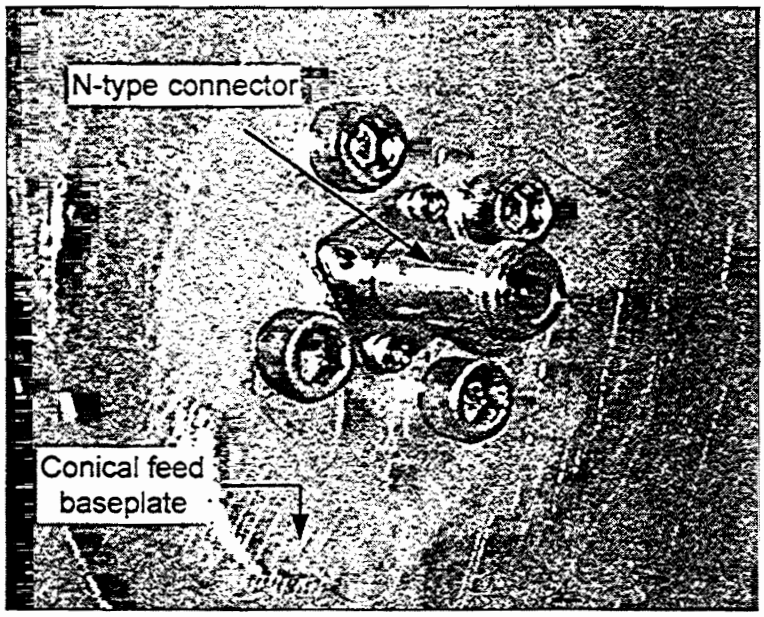

Figure 5. **The RF feed of the COBRA III. Also shown is the concial transmission line base plate.**

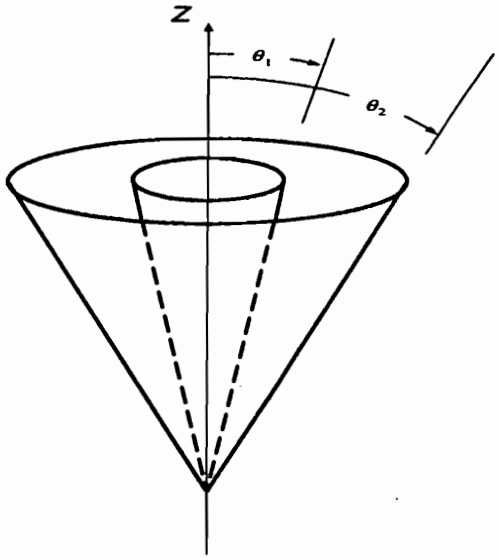

Figure 6. **The geometry of a conical transmission line. The impedance of the line is defined by the half angles of the inner and outer conductors.**

3. MEASURED INPUT IMPEDANCE OF COBRA III

The input impedance of the COBRA III is not band limited by the low frequency cutoff of a feed waveguide or feed horn. Rather, the design and quasi-TEM nature of the coaxial conical transmission line intentionally maximizes the operational bandwidth of the antenna. The input impedance of the COBRA III was measured with a Hewlett-Packard (HP) 8753 vector network analyzer (VNA) equipped with the time domain option. This section reports the results of those measurements.

3.1 Frequency and Time Domain Results

The input impedance of the COBRA III was measured at the input terminals of the COBRA III, the N-type connector (see Figure 5). The measured values of the reflection coefficient in dB, over the frequency range of 45 MHz – 6 GHz, at the input terminals of the COBRA III prototype are given in Figure 7. There, it is indicated that the return loss is approximately –5 dB or less above 100 MHz. The reflection coefficient values on a linear scale are given in Figure 8. Also indicated in Figure 8 is the standing wave ratio at the input terminals of the antenna. An average SWR ~ 3 over the 0.1 – 6 GHz bandwidth is observed.

These initial measurements included the effects of several impedance discontinuities in the COBRA III transmission line. The measurements of Figure 7 were transformed into the time domain via an internal algorithm of the HP 8753. The result is a record of the magnitude of the reflection coefficient as a function of time, as shown in Figure 9. There are four major points of impedance discontinuity in the COBRA III feed, they are: (a) the SMA to N-type connector transition; (b) the N-type 50-Ω transmission line impedance to the COBRA III internal 50-Ω transmission line transition (the portion of the transmission line that passes through the base plate); (c) the internal 50-Ω coaxial transmission line to internal 80-Ω conical transmission line transition; and (4) the location at which the center conductor of the conical transmission line attaches to the subreflector. The locations of impedance discontinuities, round-trip times of flight, and magnitudes of the reflection coefficient of the COBRA III feed are summarized in Table 2.

Table 2. The locations of impedance discontinuities, round trip times of flight, and magnitudes of the reflection coefficient of the COBRA III feed.

Impedance Discontinuity	Round trip time of flight to discontinuity (ns)	Magnitude of Reflection Coefficient
SMA to N-type connector transition at COBRA III feed point	0	0.03
N-type 50-Ω impedance to internal 50-Ω transmission line.	0.5	0.14
Internal 50-Ω to 80-Ω transmission line discontinuity	1.4	0.24
Conical transmission line and subreflector interface	3.6	0.25

3.2 Time Gating Applied to Input Impedance Measurements

Of the four major impedance discontinuities of the COBRA III listed in Table 2, only the last one is a fundamental part of the feed design. The others are artifacts of connectors and the intentional feed mismatch (i.e., the internal 50-Ω coaxial transmission line to internal 80-Ω conical transmission line transition). Using the "*time gating*" property of the HP 8753, the response of the COBRA III due to the first three impedance discontinuities can be removed mathematically. First, the VNA is directed to remove the discontinuities occurring before 2 ns. In effect, this sets the reflection coefficient = 0 for all times earlier than $t = 2$ ns. The "gated" response of the reflection coefficient at the COBRA III input terminals is shown in Figure 10. There, it is observed that the time of the major discontinuity remaining in the response is associated with the location at which the center conductor of conical transmission line attaches to the subreflector. The inverse Fourier transform is subsequently applied to the gated time domain response to yield a "gated" frequency domain response. The modified response is shown in Figure 11, where the frequency domain values of the reflection coefficient, in dB, at the input terminals of the COBRA III prototype with time gating (2-10 ns) are given. In Figure 12, frequency domain values of the reflection coefficient, in linear units, and the SWR at the input terminals of the COBRA III prototype with time gating (2-10 ns) applied are presented. One notes that, with the time gate applied and the impact of connector and impedance mismatches removed, the return loss is less than –7 dB (as shown in Figure 11). The associated SWR over the bandwidth of the measurement is 2.5 : 1 or less (as shown in Figure 12). It is obvious that the feed structure works better at the higher frequencies, as one would expect.

3.3 Correction to Measured Gain due to Impedance Mismatch

The impedance mismatch of the COBRA III referenced to its input terminals affects the measured gain values. To remove this artifact of the measurement, the power loss due to impedance mismatch is computed as follows. The square of the values of reflection coefficient (see Figure 8) are subtracted from 1; then, 10 times the log (base 10) of this value represents the power loss due to impedance mismatch in dB.

$$loss = 10\log(1-\rho^2) \text{ dB}$$

These values are given as a graph in Figure 13, and in tabular form in Table 3. For gain measurements reported as "corrected," these values are subtracted from the measured values of gain for each COBRA III configuration. These impedance measurements were taken for a particular COBRA configuration (all petals at position 0), and the assumption is that the input impedance of the COBRA III is not a function of configuration (petal position), which has been our experience.

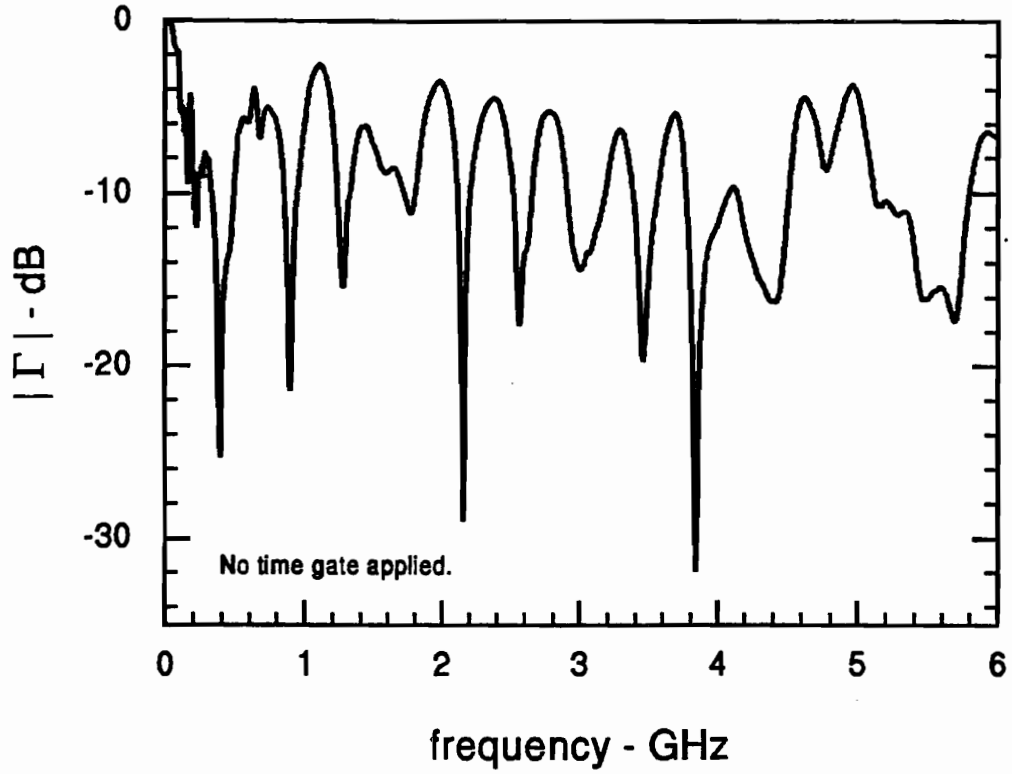

Figure 7. **The measured values of the reflection coefficient, in dB, at the input terminals of the COBRA III prototype.**

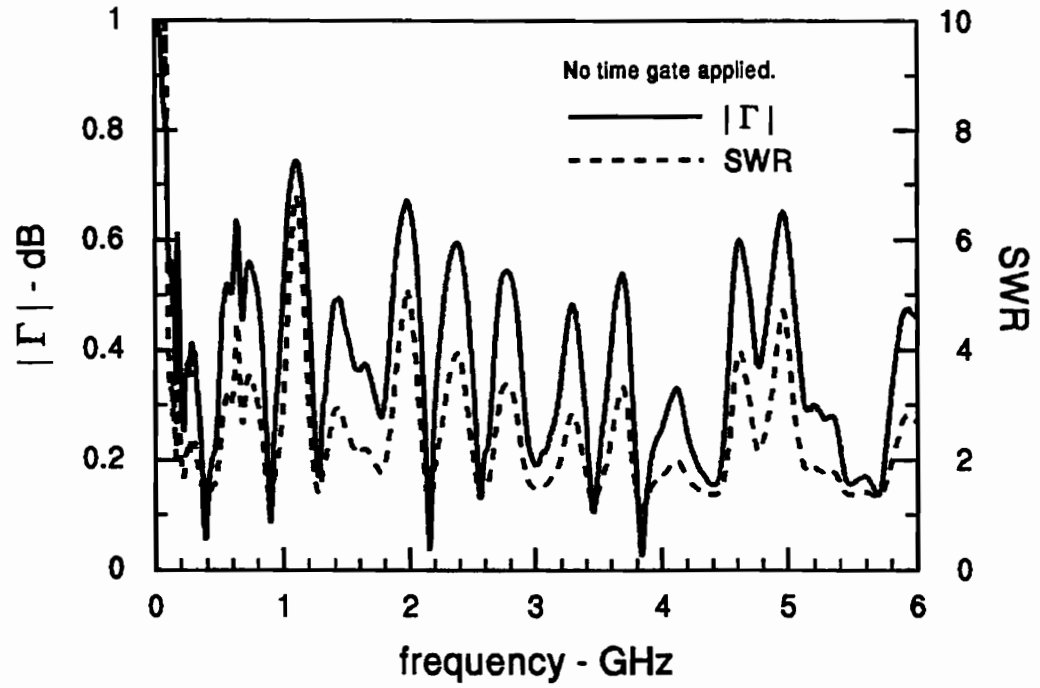

Figure 8. **The measured values of the reflection coefficient, in linear units, and the SWR at the input terminals of the COBRA III prototype.**

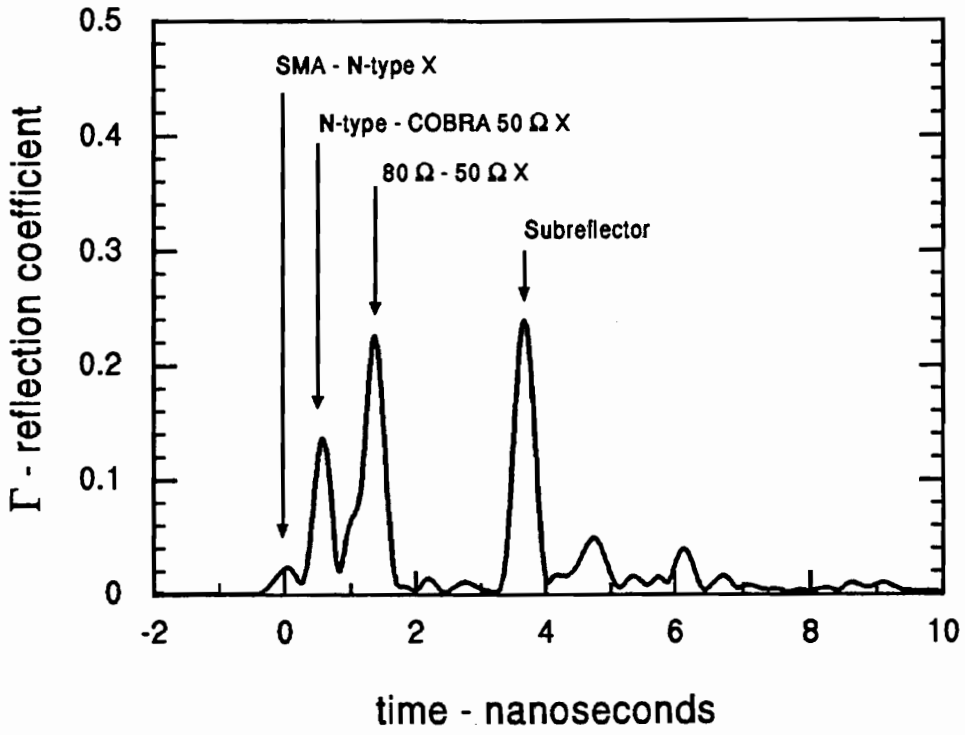

Figure 9. **The time domain response of the COBRA III. Time of flight values associated with significant impedance discontinuities are indicated.**

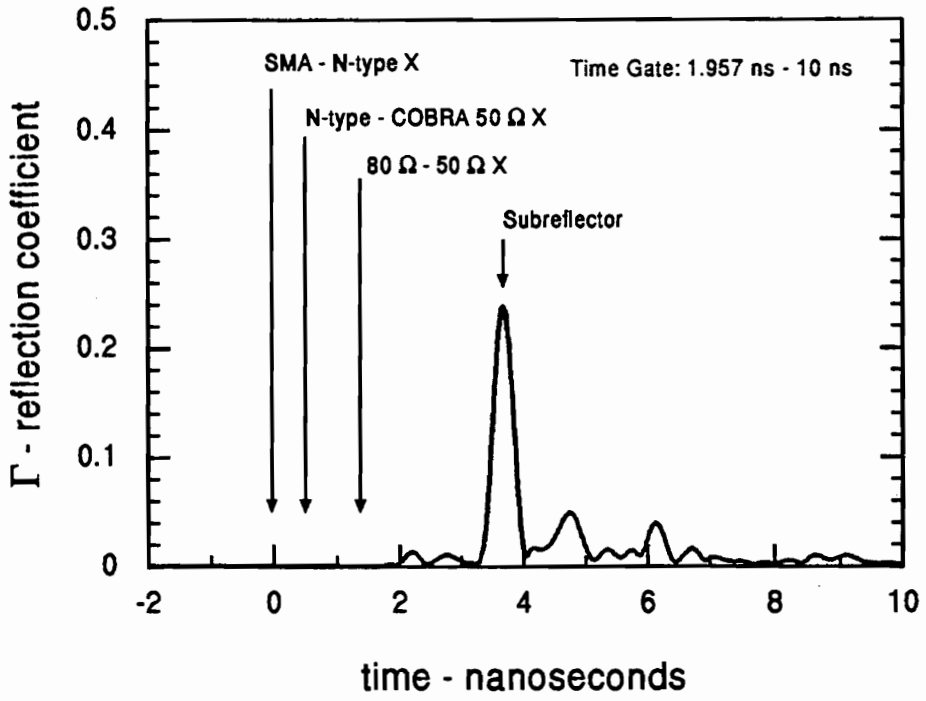

Figure 10. **The time domain response of the COBRA III with "time-gating" applied. The gate was applied around the 2 – 10 ns time period, excluding events occurring earlier in time.**

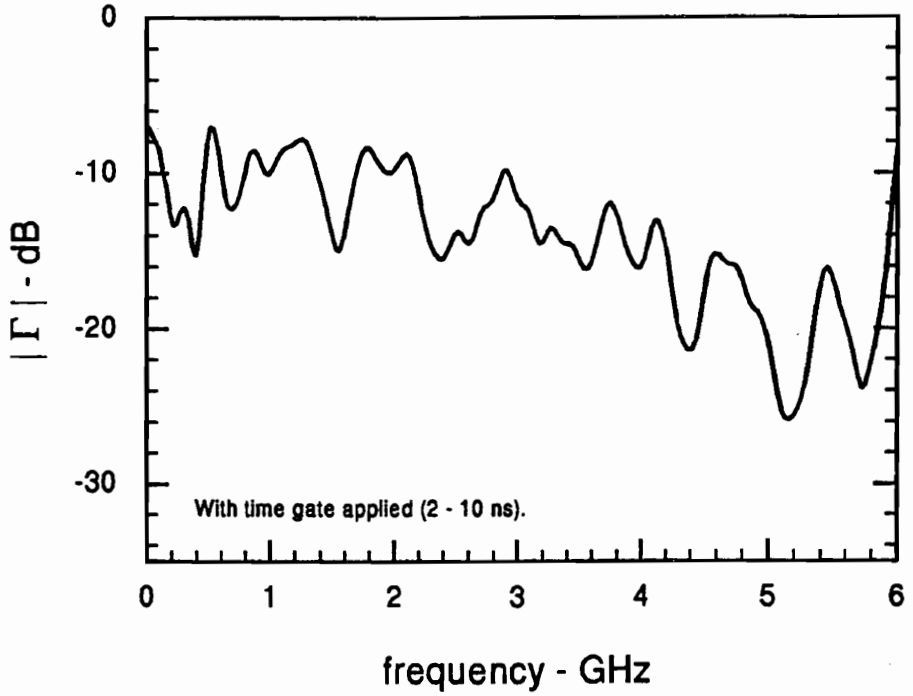

Figure 11. **Frequency domain values of reflection coefficient, in dB, at input terminals of COBRA III, with time gating (2 – 10 ns) applied.**

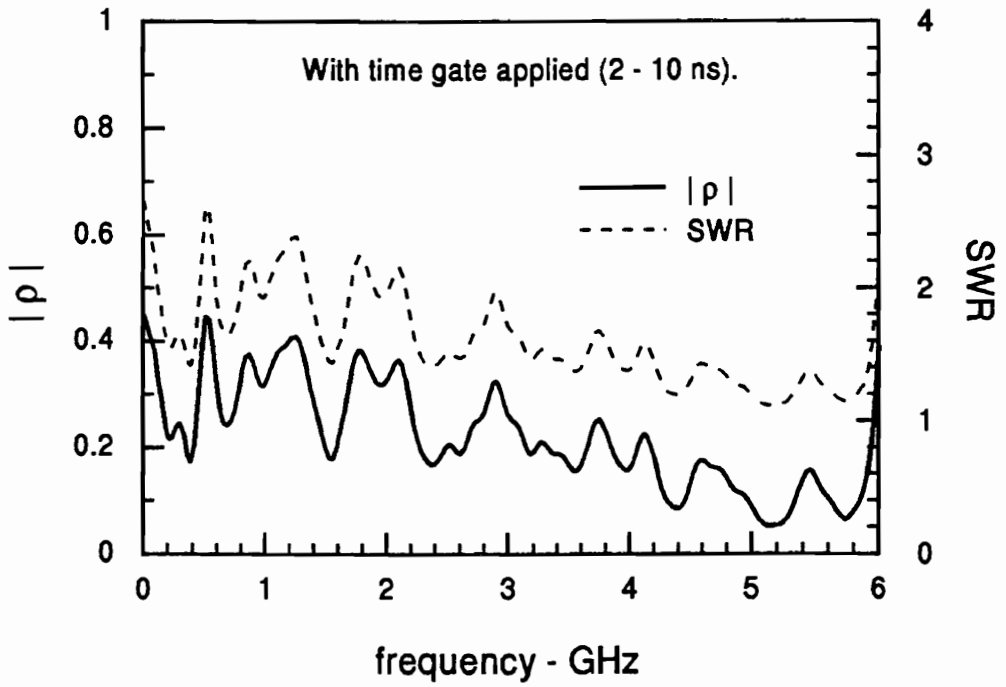

Figure 12. **Frequency domain values of the reflection coefficient, in linear units, and the SWR at the input terminals of the COBRA III prototype with time gating (2 – 10 ns) applied.**

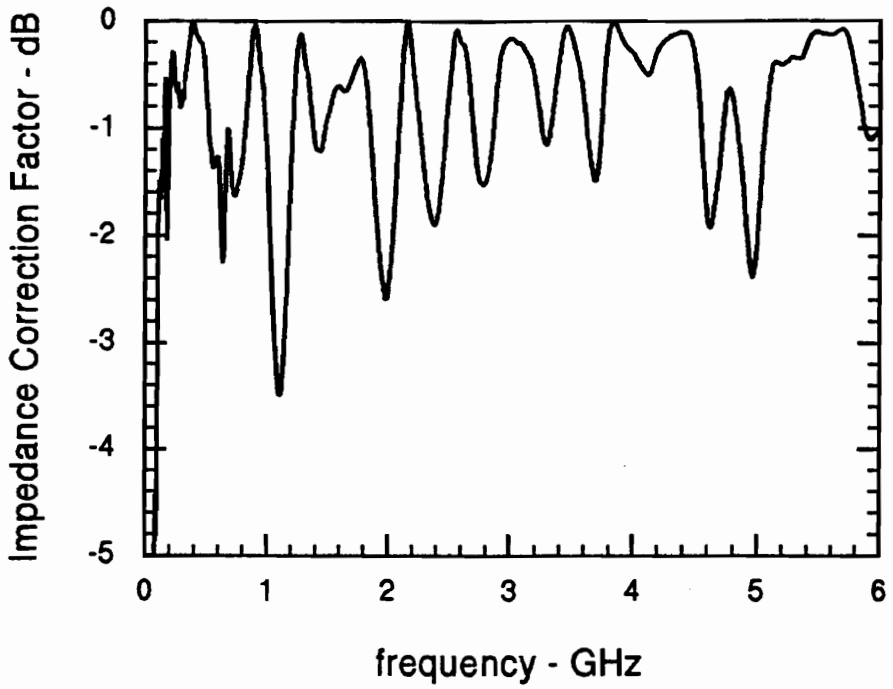

Figure 13. **The correction factors applied to measured values of gain, as a function of frequency, due to the impedance mismatch at the input terminals of the COBRA III. These values were subtracted from the "raw" measured values of gain to yield corrected gain values.**

Table 3. **The values of the gain correction factor used to account for impedance mismatch at selected frequencies across the measurement band. These values were subtracted from the "raw" measured values of gain.**

Frequency - GHz	Correction - dB
0.5	-0.711
1.0	-1.24
1.5	-0.90
2.0	-2.52
2.5	-0.66
3.0	-0.16
3.5	-0.16
4.0	-0.30
4.5	-0.36
5.0	-1.98
5.5	-0.1
6.0	-1.0

4. TEST CONFIGURATION AND PROCEDURE

The measurements of the electrical and radiating properties of the COBRA III prototype were conducted in the anechoic chamber of the High Energy Microwave (HEML) facility (Kirtland Air Force Base), over the 7 – 18 February 2000 interval. The measurements were made using the Air Force Research Laboratory's Narrowband Antenna Range system [Ref. 7, 8]. This section presents a brief overview of the antenna measurement system, a description of the system's sensors (antennas), and the results of a procedure validating gain measurement using the system.

4.1 Antenna Measurement System Overview

The Air Force Research Laboratory's (Phillips Site) Narrowband Antenna Measurement System utilizes an HP 8510C Vector Network Analyzer paired with a custom *s*-parameter test set. It can measure antenna gain over the 0.045 - 12 GHz band, and can operate over long distances. Using a pair of HP microwave frequency sources, the system exhibits a 90-dB dynamic range, and will provide up to 20 dBm (30 dBm without lock) of radiated RF power (easily amplified to higher powers). A 1-D turntable permits measurements over a full 360-degrees in azimuth. Custom software fully automates antenna position control, RF configuration of system instruments, data acquisition, data reduction, data analysis and data archival.

The system accomplishes the measurement of the absolute gain of an antenna under test (AUT) using two independent measurements, and a gain comparison technique. A system transmit (TX) antenna radiates RF power toward a suite of co-located antennas. A first measurement records the ratio of the received power of a calibration (CAL) antenna to a reference (REF) antenna. A second measurement records the ratio of the received power of an AUT to the REF antenna. It is required that the CAL antenna be a well-characterized antenna for which the frequency response (gain) is known and stored in the antenna range system database. The REF antenna must exhibit a broad response characteristic about the frequency bandwidth of interest, but absolute characterization of its gain is not required. Both the REF and CAL antennas are fixed in position and orientation throughout the measurement.

As described, the second measurement records the AUT to REF power ratio. The antenna range data reduction module then determines the ratio of the two measurements

$$\frac{AUT}{REF} / \frac{CAL}{REF} = \frac{AUT}{CAL}$$

and the AUT gain is determined by subtracting the known (calibrated) response, in dB, of the CAL antenna

$$AUT_{Gain} = \left(\frac{AUT}{REF}\right)_{dB} - \left(\frac{CAL}{REF}\right)_{dB} - CALGain_{dB}$$

A functional block diagram of the system is shown in Figure 14. The system is more complex than just described, and a full description of the system and its capabilities can be found in [Ref. 7,8]. The characteristics of the system sensors (antennas) are described in the next section.

4.2 Narrowband Antenna Measurement System Sensor Characteristics

Four antennas (sensors) are typically used with the Narrowband Antenna Measurement System. They are:

1. Antenna Under Test (AUT)—The antenna to be characterized in terms of its spatial pattern (azimuthal) and frequency dependence on gain. In this case the AUT is the COBRA III prototype.
2. Reference Antenna (REF)—The "port-two" antenna, common in both measurements needed to determine the AUT gain. In this case, the REF line was cabled directly from the transmitter, so a REF antenna was not required.
3. Calibration Antenna (CAL)—A well characterized antenna, its response is used to make an antenna comparison-type gain measurement of the AUT. In this case, both a 1492 antenna (2 – 18 GHz dual ridged horn) and a 1734 antenna (0.5 – 5 GHz dual ridged horn) were used.
4. Transmit Antenna (TX) —The antenna that radiates the RF signal used in the measurements. For this measurement, an AEL-1492, 2 – 18 GHz dual-ridged horn antenna was used.

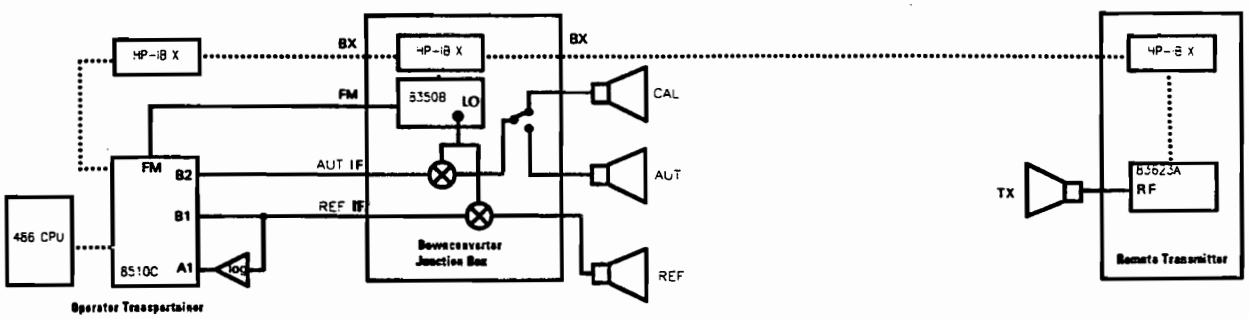

Figure 14. Functional block diagram of Narrowband Antenna Measurement system.

Transmit (TX) Antenna

An AEL-1498 dual-ridged waveguide horn antenna (2 - 18 GHz) was used as the transmit antenna during the COBRA prototype measurements. This worked well for these measurements because its bandwidth covered the 2 - 8 GHz bandwidth of interest, and its broad, low-gain radiated pattern equally illuminated the AUT and CAL antennas. Also, the AEL-1498's input impedance was well matched over the test bandwidth. The transmit antenna was separated from the AUT and CAL antennas by approximately 45 feet..

Reference (REF) Antenna

Separation between the transmit antenna and receive site was minimal, so the REF signal was cabled directly to the receive hardware. This eliminated the requirement for a fourth antenna, and the labor associated with antenna siting and alignment.

Calibration (CAL) Antenna

The calibration antenna was either a 1498 (2 – 18 GHz) or 1734 (0.5 – 5 GHz) dual-ridged horn. The gain curve for the 1498 is shown in Figure 15, and the gain curve for the 1734 is shown in Figure 16. These curves were used as the "calibration standard" against which the AUT was measured. A measurement of the gain of a 1734 was made with the antenna range system, and the resulting gain determined by the system's data reduction was compared with the 1734 calibration curve. These curves are shown overlayed in Figure 17. One notes good agreement over the overlapping range, with maximum deviation of approximately 1.5 dB.

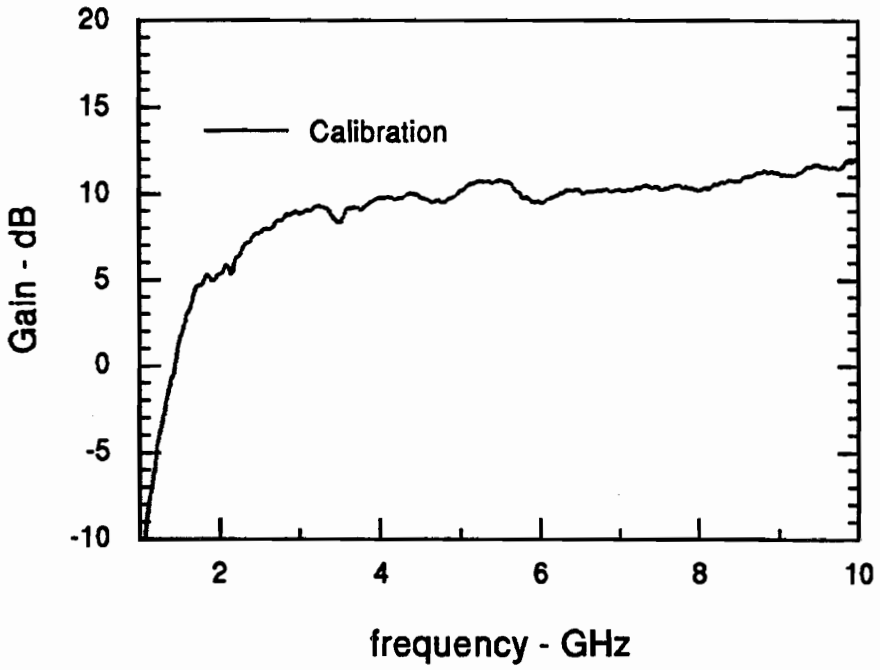

Figure 15. The gain of the 1498 dual ridged horn used as the CAL antenna.

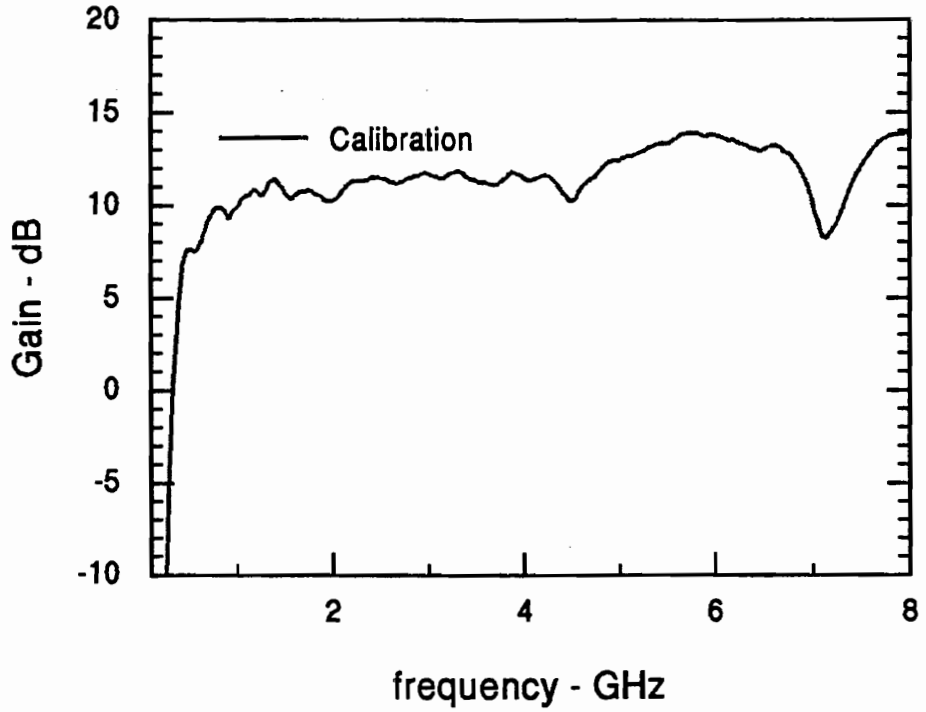

Figure 16. The gain of the 1734 dual ridged horn used as the CAL antenna.

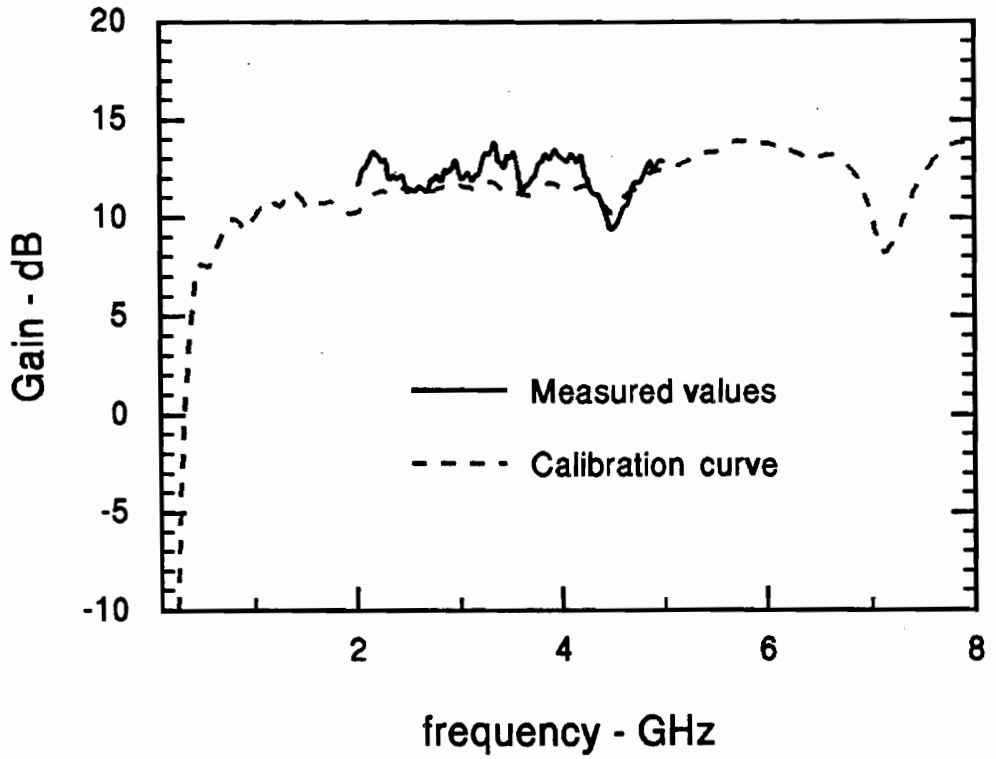

Figure 17. The measured gain of a 1734 dual ridged horn antenna, and the calibration curve determined from an independent measurement.

5. MEASURED PATTERNS OF COBRA III: N = 1

The gain and patterns of the COBRA III were measured for an N = 1 configuration. In this configuration, all petals of the antenna are at the same position (0, 1, 2 or 3). The measured pattern, at 3 GHz, of the COBRA III in the N = 1 configuration is presented in Figure 18. Shown are the azimuthal patterns corresponding to the COBRA III's response for the cases where the transmitter polarization is vertical and horizontal. Note that the response of the COBRA III is the opposite (peak gain for vertical transmit polarization) for a pattern cut in the elevation plane.

The measured peak value of the gain of the COBRA III in the N = 1 configuration was 29.2 dB. From [Ref. 10] the gain of a TM_{01} mode driven circular aperture can be approximated as

$$Gain = 20\log\left(\frac{\pi D}{\lambda}\right) - ATL - PEL + 20\log\left(\frac{1+\cos\theta_{max}}{2}\right)$$

For the present case: ATL ~ 1.09 dB; PEL ~ 3 dB; $20\log\left(\frac{1+\cos 4^\circ}{2}\right) = -0.01$ dB, and

$20\log\left(\frac{\pi D}{\lambda}\right) \approx 20\log\left(\frac{2\pi}{0.1}\right) \approx 36$ dB. Then, $Gain = 36 - 1.09 - 3 - 0.01 = 31.9$ dB, which is slightly higher than our measured result, but within a reasonable range.

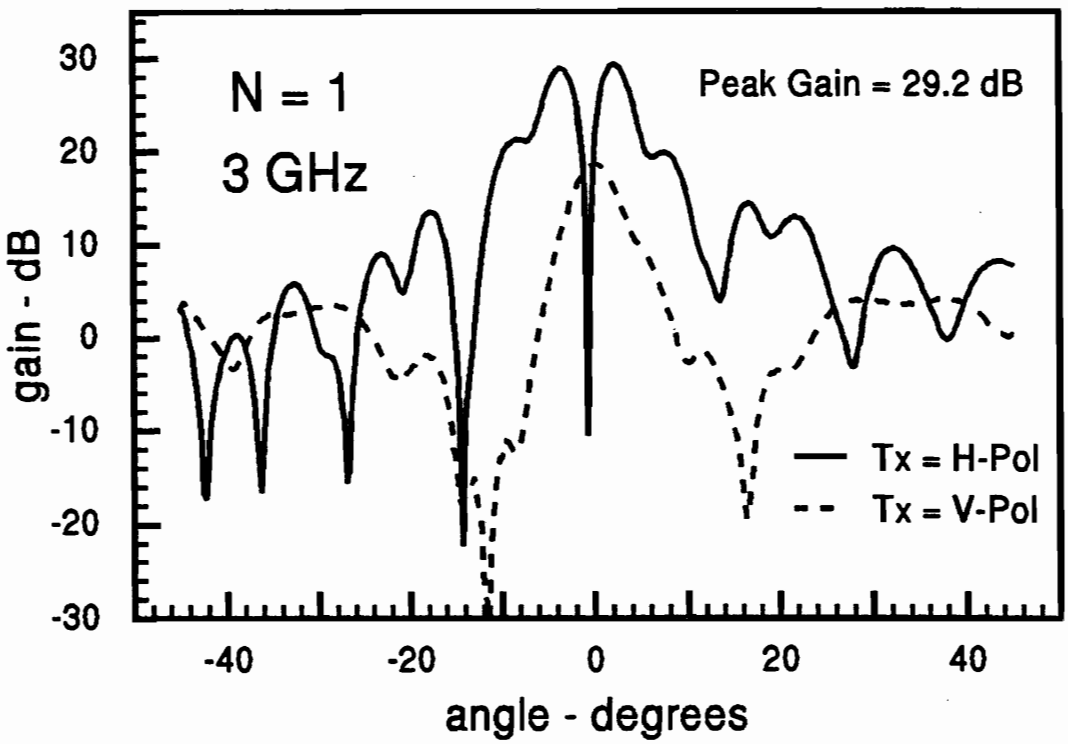

Figure 18. The measured azimuthal pattern of the COBRA III for N = 1 at 3 GHz.

6. MEASURED PATTERNS OF COBRA III: N = 2

For the N = 2 configuration, two adjacent petals are at a specified position, while the other two petals are at a position two increments away. For example, if petals I and IV are at position 1, then petals II and III would be at position 3. Consider Figure 19a which depicts a view looking into the main reflector from the front. There also the petal numbers are identified. In Figure 19b is shown (petals at indicated positions) the N = 2 configuration which produces a boresight peak with linear polarization.

To minimize the focal length error associated with the translation of the petals, one could translate the petals such that their focal points were located at equal distances in front of, and behind the original focal point of the un-cut paraboloidal reflector. As described in [Ref. 2], our approach was to add petal rotation to co-locate the focal points of the translated petals.

The measured pattern, at 3 GHz, in the azimuthal plane of COBRA III in an N = 2 configuration is shown in Figure 21. The antenna was configured such that petals I and II are at position 3, and petals III and IV are at position 1. For this configuration, the response of the antenna should be a maximum on boresight for vertically polarized excitation. The response of the antenna is shown in Figure 20 for the case where the transmit polarization is vertical, and the case where the transmit polarization is horizontal. The peak gain was found to be 29 dB, with a half power beam width of 4.5°. Again relying on an approximate formula [Ref. 11]

$$Gain \approx \frac{26,000}{HP_{E^\circ}\, HP_{H^\circ}} = \frac{26,000}{(4.5)^2} = 1,283 \rightarrow 31 \text{ dB}$$

which again is somewhat higher than our measurement, but within an acceptable range to permit confidence in the measurement.

The measured boresight gain, as a function of frequency, of the COBRA III in an N = 2 (with a peak response to vertical polarization) configuration is given in Figure 21. Note that the results have been compensated for impedance mismatch. One notes a peak response about the center frequency, 3 GHz, and a halfpower bandwidth of about 1 GHz. For these measurements the antenna was physically configured to operate at $f_0 = 3$ GHz.

The measured pattern, at 3 GHz, in the azimuthal plane of COBRA III in an alternate N = 2 configuration is shown in Figure 22. The antenna was configured such that petals I and IV are at position 3, and petals II and III are at position 1. For this configuration, the response of the antenna should be a maximum on boresight for horizontally polarized excitation. The response of the antenna is shown in Figure 22 for the cases where the transmit polarization is vertical and horizontal. The peak gain is found

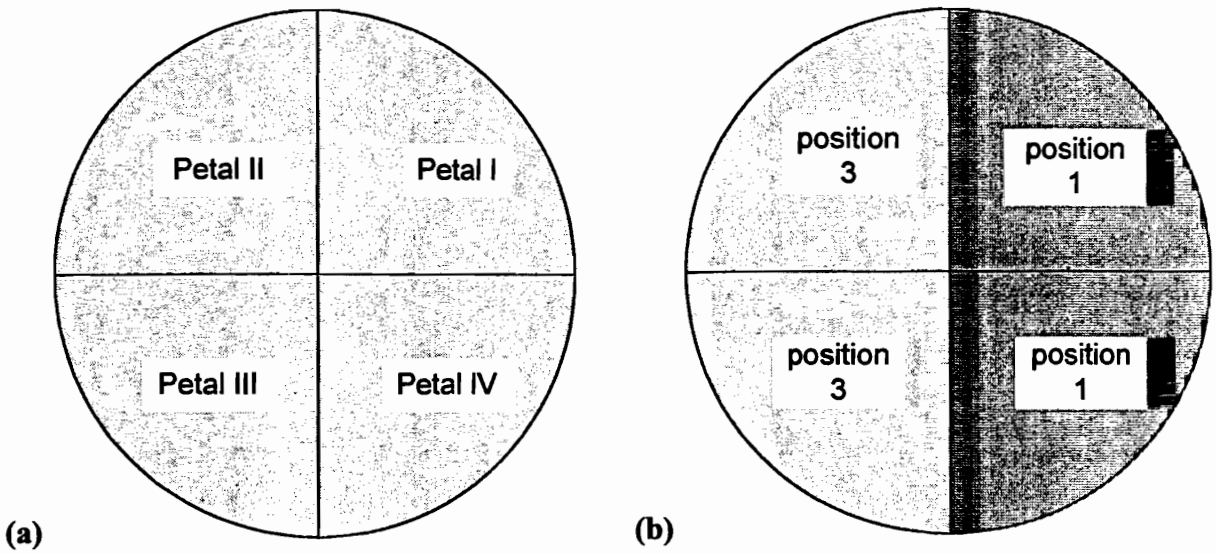

Figure 19. Petal configuration: (a) looking into the main reflector from the front, the petals are identified; and (b) shown (petals at indicated positions) is the N = 2 configuration, which produces a boresight peak with linear polarization.

to be 29.5 dB, with a half power beam width of 3.5°. Once again relying on the approximate formula

$$Gain \approx \frac{26{,}000}{HP_{E^\circ}\, HP_{H^\circ}} = \frac{26{,}000}{(3.5)^2} = 2{,}122 \rightarrow 33.3 \text{ dB}$$

The measured result is lower than this estimate, but the high side lobes somewhat invalidate this approximation.

The measured boresight gain, as a function of frequency, of the COBRA III in an N = 2 (with a peak response to horizontal polarization) configuration is presented in Figure 23. Again, note that the results have been compensated for impedance mismatch. The peak response is about at the center frequency, 3 GHz, and a half power bandwidth of about 1.5 GHz is seen. Again, the antenna was configured to operate at $f_0 = 3$ GHz for these measurements.

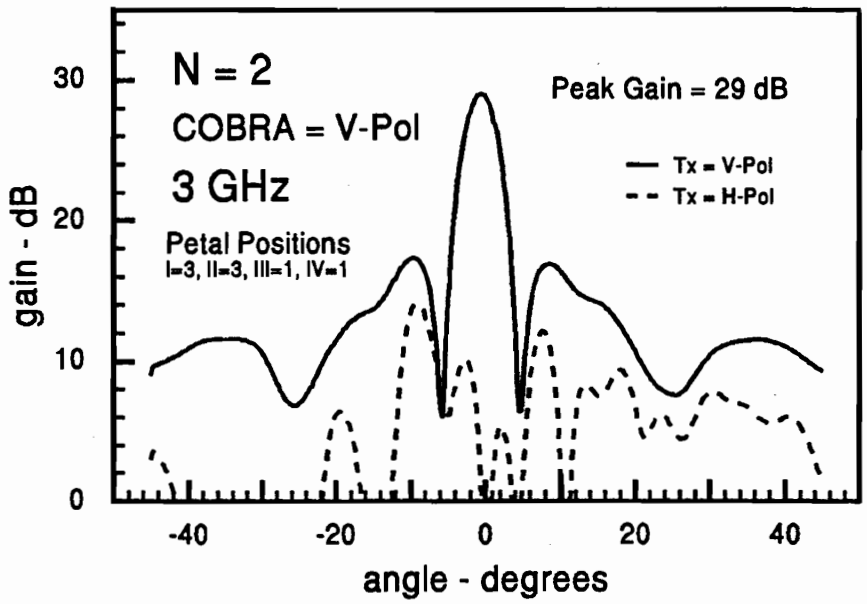

Figure 20. **Measured pattern, at 3 GHz, in the azimuthal plane, of COBRA III in an N = 2 (with a peak response to vertical polarization) configuration. Response shown for the cases where transmit polarization is vertical and horizontal.**

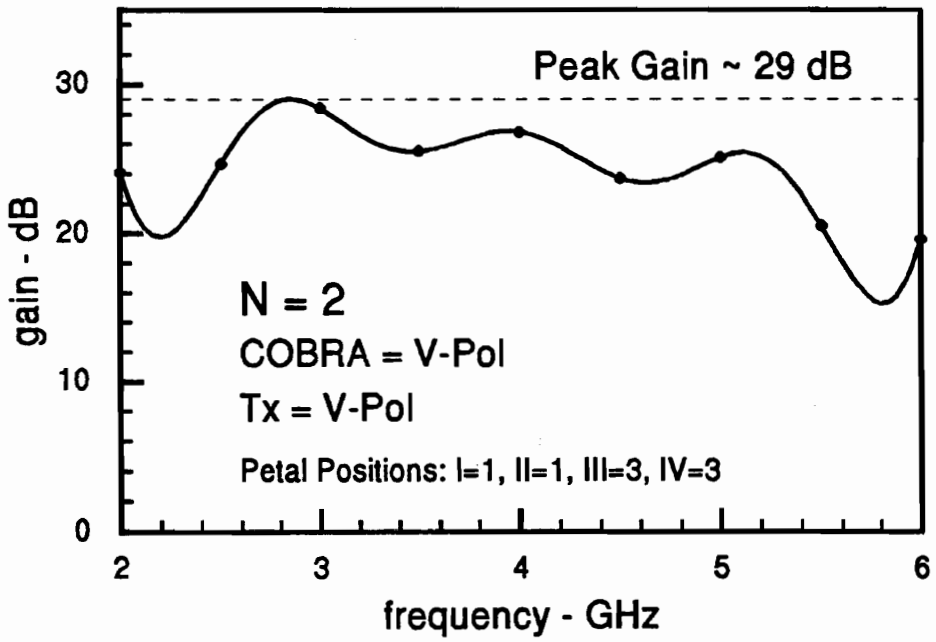

Figure 21. **The measured boresight gain, as a function of frequency, of the COBRA III in an N = 2 (with a peak response to vertical polarization) configuration. Results have been compensated for impedance mismatch, and the antenna was configured to operate at $f_0 = 3$ GHz.**

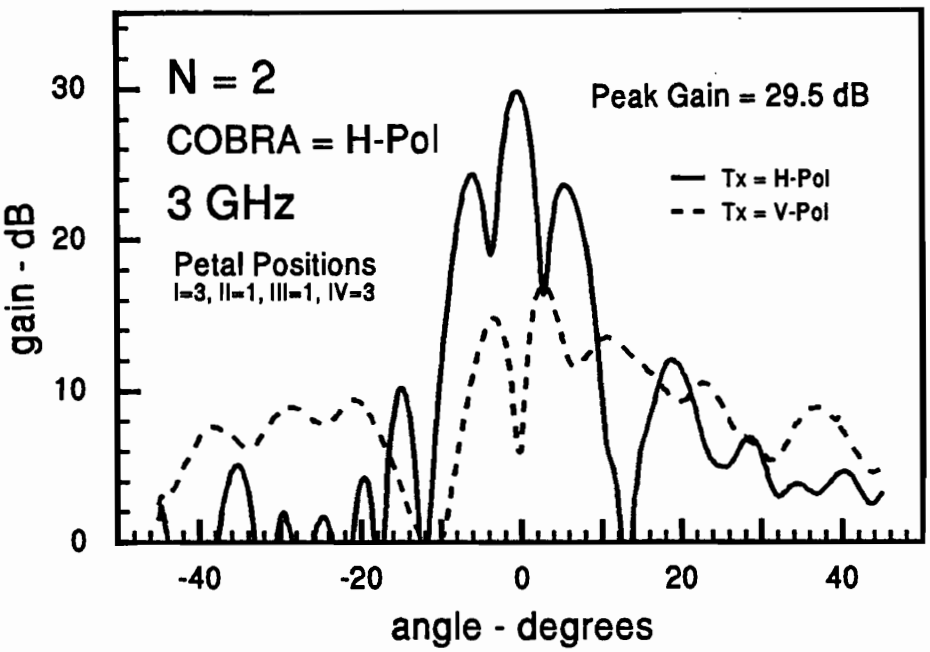

Figure 22. **Measured pattern, at 3 GHz, in the azimuthal plane of COBRA III in an N = 2 (with a peak response to horizontal polarization) configuration. The response of the antenna is shown for the cases where the transmit polarization is vertical and horizontal.**

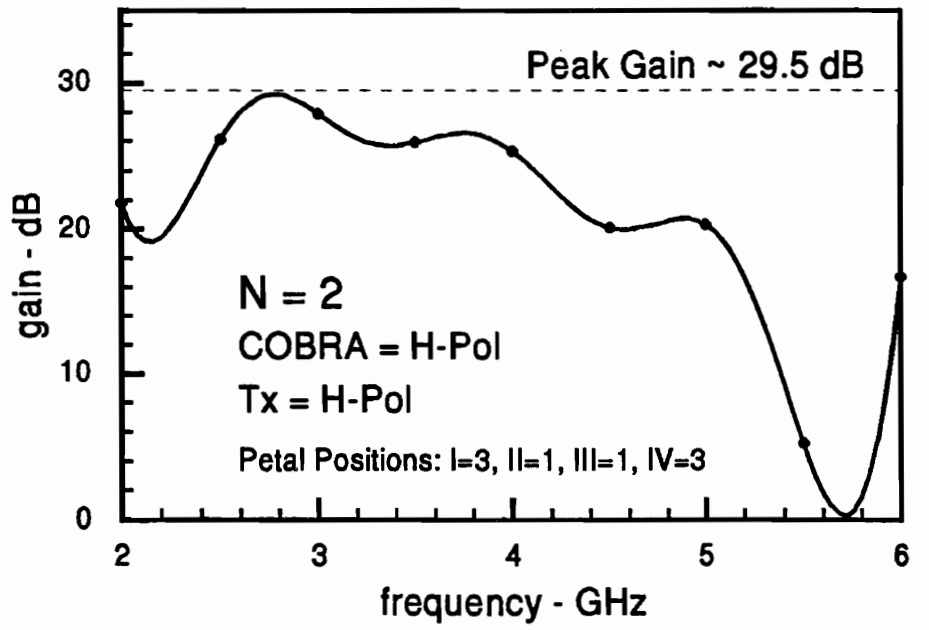

Figure 23. **The measured boresight gain, of the COBRA III in an N = 2 (with a peak response to horizontal polarization) configuration, as a function of frequency. Results have been compensated for impedance mismatch, and the antenna was configured to operate at $f_0 = 3$ GHz.**

7. MEASURED PATTERNS OF COBRA III: N = 4

For the N = 4 configuration, adjacent petals are offset from one another by a single position increment in a monotonically increasing or decreasing fashion. For example, if petal I is at position 0, then petals II, III and IV are at positions 1, 2 and 3 respectively. Consider Figure 24a which depicts a view looking into the main reflector from the front. In Figure 24b is shown (petals at indicated positions) an N = 4 configuration which produces a boresight peak with circular polarization from an azimuthally symmetric feed excitation. Note that many permutations of this arrangement will also yield an N = 4 configuration.

The measured pattern, at 3 GHz, in the azimuthal plane of COBRA III in an N = 4 configuration is shown in Figure 25. The antenna was configured such that petal I is located at position 0, while petals II, III and IV are at positions 1, 2 and 3 respectively. For this configuration the response of the antenna should be a maximum on boresight for circularly polarized incident field. The response of the antenna is shown in Figure 25 for the case where the transmit polarization is vertical. The peak gain was found to be 26.5 dB, with a half power beam width of 4.1°. The response of the antenna for the case where the transmit polarization is horizontal is also shown in Figure 26. The peak gain was found to be 26 dB, with a half power beam width of 3.25°. The measured boresight gain, as a function of frequency (2 – 6 GHz), of the COBRA III in an N = 4 configuration (transmit antenna is vertically polarized) is shown in Figure 27. The half power bandwidth is approximately 1 GHz. The measured boresight gain, as a function of frequency, of the COBRA III in an N = 4 configuration (transmit antenna is horizontally polarized) is given in Figure 28. The half power bandwidth is approximately 1.7 GHz (2.5 – 4.2 GHz). Results have been compensated for impedance mismatch, and for these measurements the antenna was configured to operate at $f_0 = 3$ GHz.

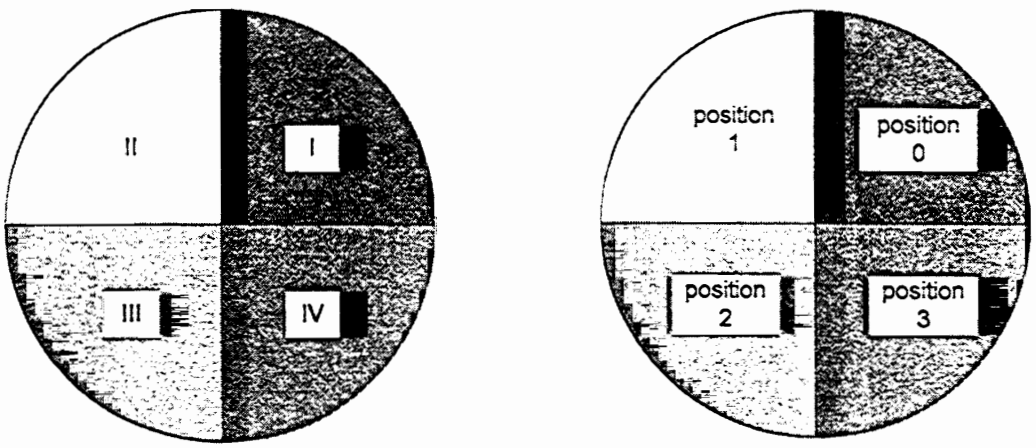

Figure 24. Petal configuration: (a) looking into the main reflector from the front, the petals are identified; and (b) shown (petals at indicated positions) is the N = 4 configuration, which produces a boresight peak with circular polarization.

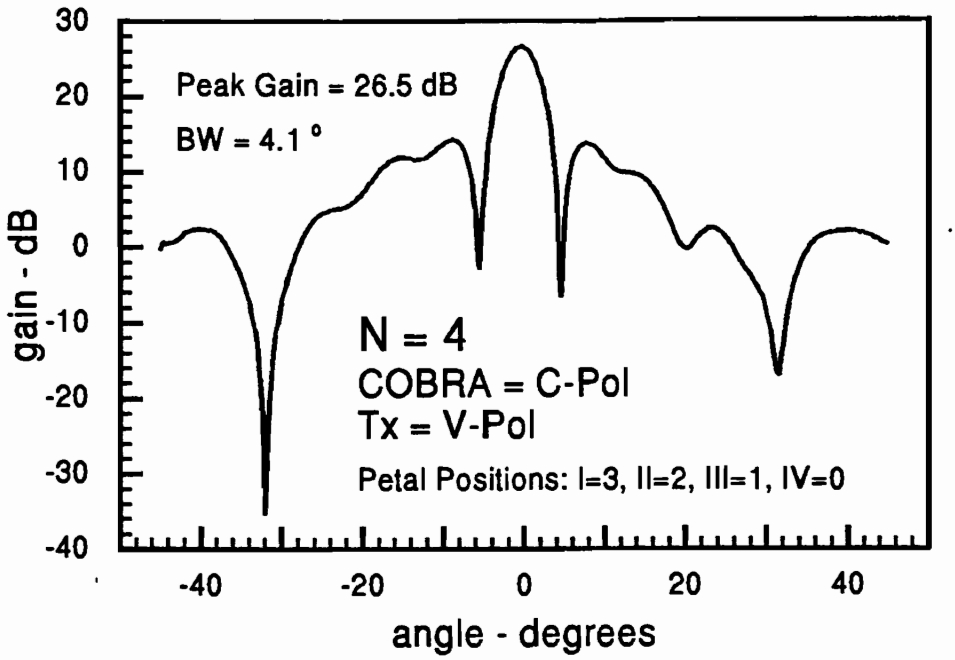

Figure 25. **Measured pattern, at 3 GHz, in the azimuthal plane of COBRA III in an N = 4 (corresponding to circular polarization) configuration. The response of the antenna is shown for the case where the transmit polarization is vertical.**

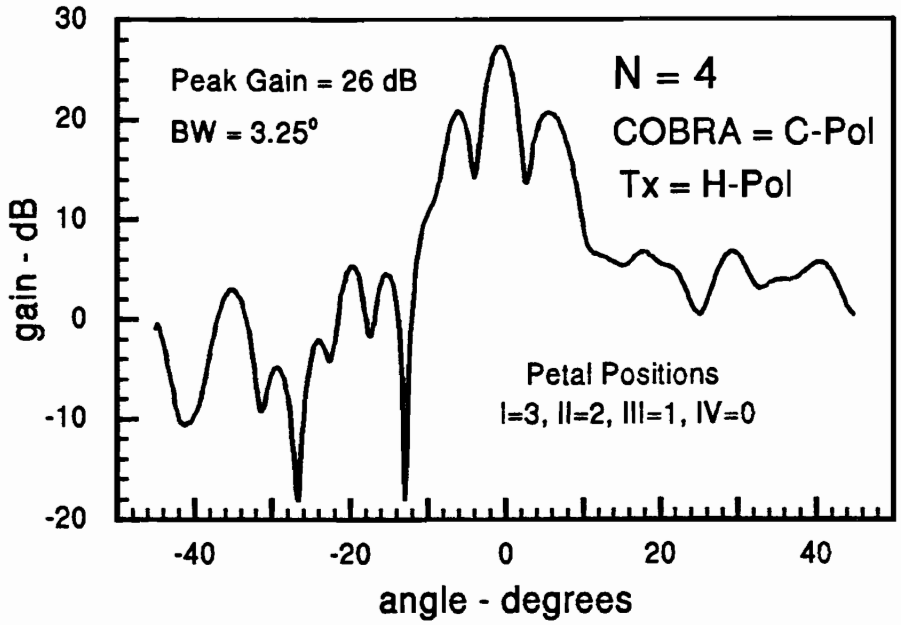

Figure 26. **Measured pattern, at 3 GHz, in the azimuthal plane of COBRA III in an N = 4 (corresponding to circular polarization) configuration. The response of the antenna is shown for the case where the transmit polarization is horizontal.**

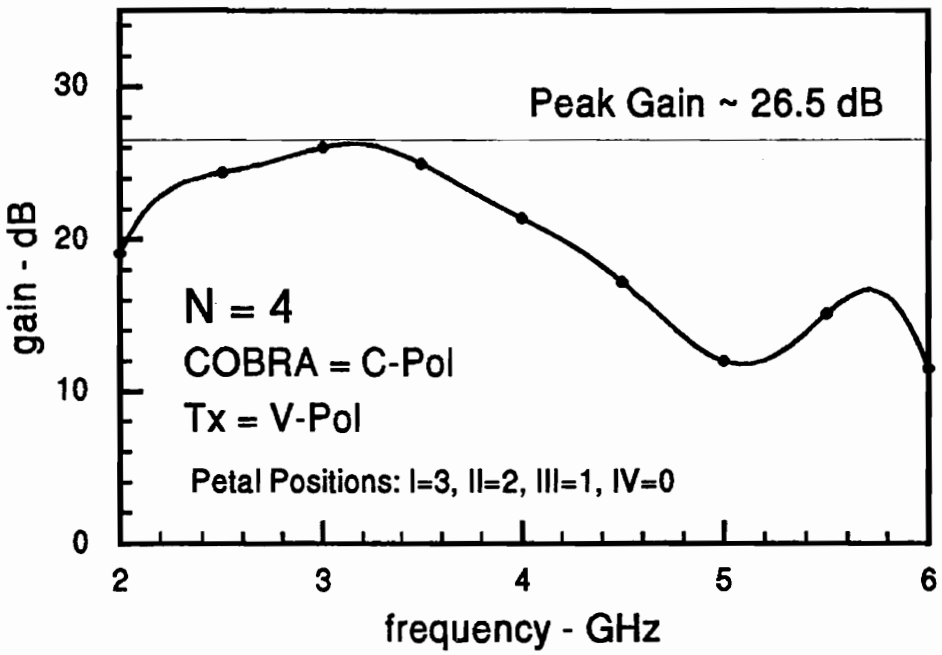

Figure 27. **Measured boresight gain, as a function of frequency, of COBRA III in an N = 4 configuration (transmit antenna is vertically polarized). Results have been compensated for impedance mismatch, and for these measurements the antenna was configured to operate at $f_0 = 3$ GHz.**

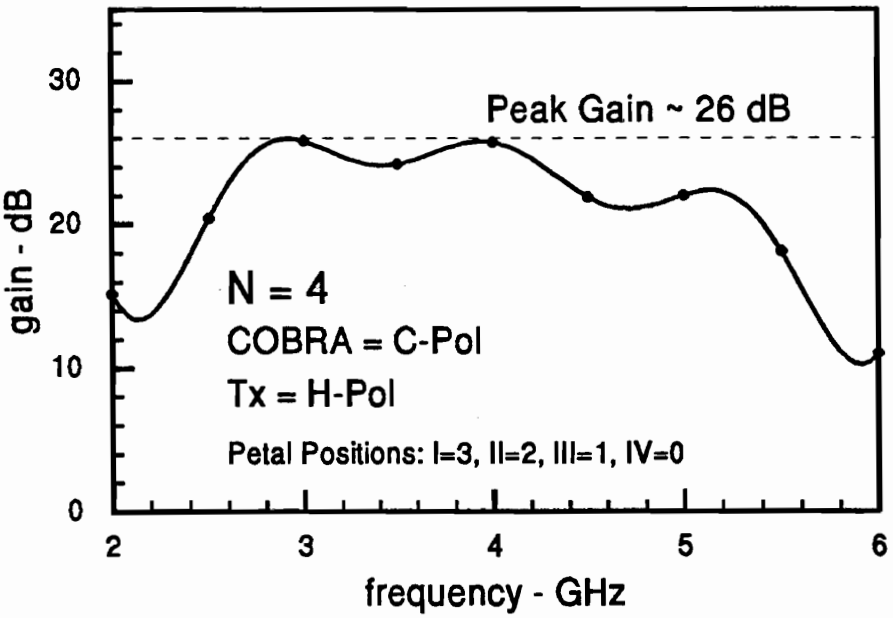

Figure 28. **Measured boresight gain, as a function of frequency, of the COBRA III in an N = 4 configuration (transmit antenna is horizontally polarized). Results have been compensated for impedance mismatch, and for these measurements the antenna was configured to operate at $f_0 = 3$ GHz.**

8. BORESIGHT MAGNITUDE AND PHASE OF COBRA III: N = 4

Measurements of the azimuthal patterns of both N=4 configuration polarizations (including the boresight gain) have shown that their peak boresight gains are approximately 26 dBi. This is consistent with the predicted circularly polarized nature of the boresight field of the N=4 configuration; however, it is not a sufficient condition to guarantee a circularly polarized boresight field. In addition, the phase difference between the two polarizations should be 90°. Depending on the reference, one polarization should lead or lag the other polarization by 90°, with the two possibilities constituting left- or right-hand circular polarization. Measurements were made to determine the phase relationship of the orthogonal components of the radiated boresight field of the N=4 COBRA. In this section, the measurement technique is described, then the measurement results are presented.

8.1 Circular Polarization Measurement Procedure

The standard Narrowband Antenna Measurement System configuration is not convenient for vector, phase-referenced measurements of two independent quantities (the magnitude and phase of the two linear polarizations of the assumed circularly polarized COBRA (N = 4) boresight field). But with a manual operating procedure and slight modifications in the manner in which the antennas (AUT, REF, TX and CAL) are connected to the system, a phase-referenced measurement of the boresight characteristic is possible with the system hardware.

To begin, the TX antenna was mounted on a piece of circular fiberglass. The CAL antenna was not used during this measurement, and the REF line was cabled directly to the receive side (as before). The fiberglass mount for the TX antenna was drilled in four places along its perimeter at equiangular intervals. The antenna was attached to the fiberglass post with two nylon screws, and mounted to the tripod with a tripod mounting grip. This permitted the antenna to be rotated 90° very accurately, without adjusting the tripod heads or physically moving the tripods (thus accurately maintaining the TX / AUT separation). This was important given the wavelength of the center frequency (λ = 10 cm at 3 GHz), and the objective of measuring relative phase to single digit degree accuracy (0.027 cm/deg.). For the first measurement, the transmit polarization was *vertical*. The HP8510 controller was placed in manual mode (from the front panel), and set to sweep across the 2 - 4 GHz bandwidth. The transmit power was set to 10 dBm, and 801 sampling points across the band was specified. A measurement sweep was conducted (magnitude and phase), and the data downloaded onto a floppy disk.

Next, the TX antenna was removed from its tripod. The fiberglass post was removed from the circular pad, rotated 90°, then re-attached. The antenna was returned to the tripod. For the second measurement, the transmit polarization was *horizontal*. A second sweep and measurement of magnitude and phase was conducted, and the display data again were downloaded onto a floppy disk.

The key to this measurement technique is to make the measurements within the smallest possible time interval. The measurement depends on the Antenna Measurement System's frequency sources phase stability over the time interval associated with the two measurements. For this reason, the measurements are made as quickly as possible, and the frequency sources on the transmit and receive sides are not turned off between measurements. We have found the phase stability of the RF frequency sources to be sufficient for these measurements.

8.2 Measured Magnitude and Phase of the N = 4 COBRA III

The COBRA III antenna was placed in an N = 4 configuration with $f_0 = 3$ GHz. The data taken from the HP8510 controller were processed to yield relative magnitude and phase (absolute phase difference between the REF line and the AUT signal) for each measurement. In Figure 29 is shown the magnitude (relative) variation of the measurement as a function of frequency for both vertical and horizontal polarization. One notes a definite frequency dependence on the received signal, but the real interest is in the differences between the magnitude of the received signal of the two polarizations. In Figure 29a is also shown the differences between the magnitude of the antenna's response subject to vertical and horizontal polarization. For perfect circular polarization, the difference between the two measurements should be 0 dB, but the difference is 1.42 dB at the center frequency ($f_0 = 3$ GHz). The difference goes to zero at a slightly higher frequency, indicating a possible slight misalignment of the antenna. The difference in the boresight gain for vertically and horizontally polarized excitation is somewhat larger than that measured earlier. This difference is blamed on antenna configuration (change of petal positions) and measurement error. Figure 29b shows the phase (relative) response variation of the COBRA III as a function of frequency for the cases where the transmit antenna is vertically and horizontally polarized. The phase difference between the two at the center frequency is 91.5°, just 1.5° from the desired 90°.

Table 4 summarizes the measurement data. There, the differences in the phase and magnitudes of the two linear polarizations are indicated for selected frequencies across the measurement band. One notes that the antenna response is remarkably broadband across the entire measurement bandwidth in terms of phase. The phase deviates from the ideal by only 21° at a maximum over the bandwidth. The half-power bandwidth is presented to be approximately 1.5 GHz.

Table 4. Summary of boresight polarization characteristics of COBRA III, configured as N=4. The center frequency of COBRA III was 3 GHz.

Frequency - GHz	Δφ	Δ-magnitude (dB)
2.0	78.9°	6.5
2.5	83.7°	3.89
3.0	91.5°	1.42
3.5	95.9°	1.11
4.0	112°	3.80

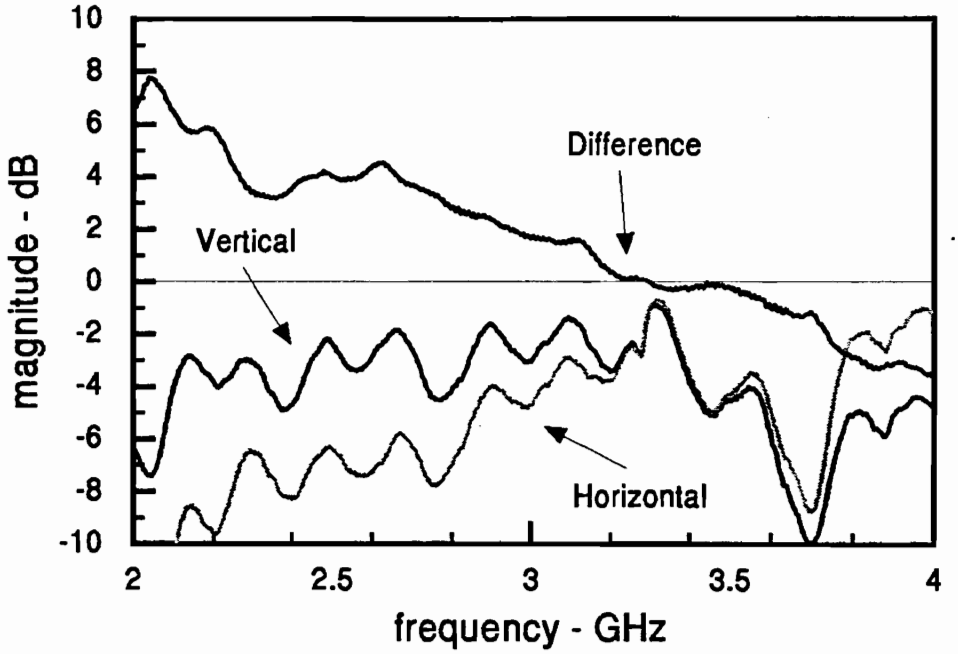

(a)

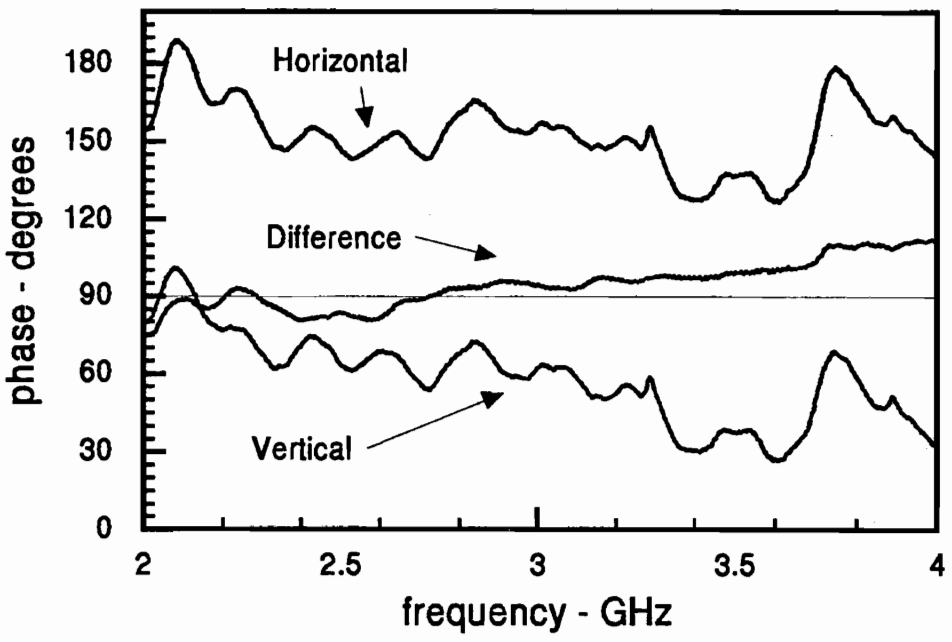

(b)

Figure 29. **Measured boresight characteristics for the case where the COBRA III is configured for circular polarization (N = 4): (a) magnitude (in dB) of antenna's response when Illuminated by vertically and horizontally polarized fields; and (b) COBRA III antenna's phase response. Differences are also indicated. The COBRA III was physically configured to have a center frequency = 3 GHz.**

9. SUMMARY, CONCLUSIONS, AND RECOMMENDATIONS

The fully illuminated aperture gain of the COBRA III is

$$G_{aperture} = 4\pi \frac{Area}{\lambda^2}$$

where the area of the COBRA III aperture is

$$\begin{aligned} Area &= \pi \left(r_2^2 - r_1^2\right) - Area_{cut\ out} \\ &= \pi \left(r_2^2 - r_1^2\right) - \left[(62.5 \times 1 \times 2) \left(\frac{2.54\ cm}{in}\right)^2 \left(\frac{1\ m}{100\ cm}\right)^2\right] = 1.6752\ m^2 \end{aligned}$$

which is less the blockage area of the subreflector (shadow), and $Area_{cut\ out}$ = an approximation of the cross sectional area lost due to segmentation of the main reflector. Then, at 3 GHz, the aperture gain is

$$G_{aperture} = 4\pi \frac{Area}{\lambda^2} = \frac{4\pi}{(0.1)^2}(1.6752) = 2{,}105 \rightarrow 33.23 \text{ dB}.$$

The aperture efficiency is defined as the ratio of the peak gain to the fully illuminated gain of the aperture. The aperture efficiencies as a function of different COBRA III configurations are summarized in Table 5.

Table 5. Summary of the peak gain and aperture efficiency associated with different COBRA III configurations, and comparison with the COBRA II measured parameters.

N	COBRA Pol	Tx Pol	COBRA II				COBRA III			
			Peak Gain		ε_A		Peak Gain		ε_A	
			Num	dB	L	C	Num	dB	L	C
1	x	H	447	26.5	21%	x	832	29.2	40%	x
2	V	V	501	27	24 %	x	794	29	38%	x
2	H	H	631	28	30%	x	891	29.5	42%	x
4	C	V	251	24	12%	24%	447	26.5	21%	42%
4	C	H	224	23.5	11%	21.2%	398	26	19%	38%

The aperture efficiency is given as ε_A-L, and as ε_A-C. These are measures of the efficiencies in terms of total received power, and indicate the aperture efficiency for linearly and circularly polarized plane wave excitation respectively. The measured values of aperture efficiencies of the COBRA III exceed the aperture efficiencies measured for

the COBRA II prototype, a standard conical horn-fed, Cassegrain configuration [Ref. 2]. Direct comparisons of the measured gain characteristics of the COBRA II and COBRA III for like configurations is presented in Table 5. The improved (over the COBRA II) gain results exhibited by the COBRA III could be due to one or more factors, including: a greater degree of optical alignment; less RF spill over at the sub-reflector due to the feed structure; and a greater degree of mechanical alignment.

Based on the measurements of the input impedance of the COBRA III prototype (see Figure 12), the bandwidth of the feed structure is less than 2.5 : 1 from 100 MHz – 6 GHz. This result was achieved by artificially removing the effect of the 50 Ω - 80 Ω discontinuity in the feed. We recommend further study, design and measurement of the COBRA III feed. This includes: (1) design, fabrication and measurement of a 50 Ω - 80 Ω adiabatic transformer; (2) design, fabrication and measurement of a feed with a 50 Ω system impedance; and (3) the design, fabrication and measurement of a conical coaxial feed and antenna with $\mathbf{p} \times \mathbf{m}$ compensation [Ref. 12] to further improve the bandwidth and gain of the antenna at lower frequencies.

The limited time available in the measurement facility necessitated a prioritization of the possible measurement tasks. The most interesting measurement yet to be taken is how well the COBRA III performs at other center frequencies, i.e., $f_0 \neq 3$ GHz. We suggest further measurements of the radiating properties of the antenna for cases where the petal positions of the COBRA III are configured for center frequencies from 100 – 1000 MHz. These would include pattern and gain measurements of the COBRA III when mechanically adjusted for a center frequency of $f_0 \neq 3$ GHz.

In conclusion, we found the operation of the Conical Transmission-Line Fed, Cassegrain Coaxial Beam-Rotating Antenna, the COBRA III, to be quite satisfactory. In terms of its measured gain, impedance bandwith and aperture efficiency, the COBRA III met or exceeded the performance of previously measured COBRA prototypes. Furthermore, we found that the design principles and guidelines developed previously [Ref. 3, 4] were valid in the design of the COBRA III. The ability to feed the COBRA directly from a coaxial transmission line, and the ability to adjust the center frequency of operation of the antenna (by physically moving petals or other reflecting surfaces) offers the possibility of extremely broadband operation. This capability may one day replace complicated parabolic dish feed structures that currently exist in communication and radio astronomy applications.

REFERENCES

1. C. Courtney and C. Baum, "Coaxial Beam-Rotating Antenna (COBRA) Concepts," Sensor and Simulation Note No. 395, April 1996.
2. C. Courtney et al., "Design and Measurement of a Cassegrain-type Coaxial Beam-Rotating Antenna," Sensor and Simulation Note No. 427, November 1998.
3. C. Courtney et al., "Design and Optimization of a Conical Transmission-Line Feed for a Coaxial Beam-Rotating Antenna," Sensor and Simulation Note No. 429, September 1998.
4. W. Prather et al., "Design and Measurement of a Conical Coaxial Transmission Line–Fed Coaxial Beam-Rotating Antenna," URSI Commission E: High Power Electromagnetics, Boulder, CO, Jan. 1999.
5. C. Courtney et al, "Considerations for a GW-level COBRA Antenna Design," Eighth National Conference on High Power Microwave Technologies, Johns Hopkins University, April 8 – 10, 1997.
6. K. Hendricks et al., "Increasing the RF energy per Pulse of an RKO," IEEE Trans. on Plasma Science, vol. 26, no. 3, June 1998.
7. "Narrow Band Continuous Wave RF Diagnostic and Data Reduction System – Software User's Manual," VS-610, Voss Scientific, December 1996.
8. "Enhanced Antenna Range System," VS-313, Voss Scientific, January 1994.
9. Clifton C. Courtney, David Slemp, Darren Baum, Carl E. Baum, Robert Torres and William Prather, "Coaxial Beam-Rotating Antenna (COBRA) Prototype Measurements," Sensor and Simulation Note No. 408, July 1997.
10. T. Milligan, *Modern Antenna Design*, p. 200, McGraw-Hill, NY, 1985.
11. W. Stutzman and G. Thiele, *Antenna Theory and Design*, p. 397, Wiley, NY, 1981.
12. M. Vogel, "Low frequency compensation of an extreme bandwidth TEM horn and lens IRA," Sensor and Simulation Note No. 391, February 1996.
13. C. Courtney and C. Baum, "The Coaxial Beam-Rotating Antenna (COBRA): Theory of Operation and Measured Performance," accepted for publication in IEEE Trans. on Antennas and Propagation, vol. 48, no. 2, February 2000.